*URSI AP-RASC 2019, New Delhi, India; 09 - 15 March 2019*

# Measurement-Based Characterization of Non-Stationary Indoor Small-Scale Fading

Evgenii Vinogradov[(1)] and Claude Oestges[(2)]
(1) KU Leuven, Department of Electrical Engineering - ESAT, Leuven Belgium
(2) Institute for Information and Communication Technologies, Electronics and Applied Mathematics (ICTEAM), Université catholique de Louvain, 1348 Louvain-la-Neuve, Belgium

## Abstract

In this work, we investigate small-scale fading observed in a singe-input-multiple-output indoor communication channel. We propose a framework to define the stationarity period and then we analyze the variations of small-scale fading statistics using the so-called second-order scattering fading (SOSF): (i) minimum stationarity period is 0.8 s, ii) the parameters of the SOSF distribution turn out to be following a Beta or an Extreme Value distribution, (iii) for describing the sudden changes of the statistics, we extracted probability and transition matrices, iv) angles of arrival can be described by a bi-modal Tikhonov-Von Mises distribution.

## 1 Introduction

A recently published white paper [1] reports that, in 2016, the monthly mobile traffic was 7.2 Exabytes and Cisco forecasts 49 Exabytes per month of mobile data traffic by 2021. Indoor environments are in the focus of multiple research in channel characterization and modeling. Moreover, the frequency band of 3.4-4.2 GHz is one of the first bands considered for the 5th generation (5G) communication networks. In [2], peer-to-peer channels were investigated in a typical US office environment, consisting in a large indoor area containing individual cubicle-style offices. A Single-Input Single-Output (SISO) channel for a typical European environment was characterized in [3]. However, Multiple-Input Multiple-Output (MIMO) properties of a non-stationary radio channel are of interest for the research and engineering community. In this paper, we investigate narrowband Single-Input Multiple-Output (SIMO) Small-Scale Fading (SS fading) based on a wideband experimental campaign at 3.8 GHz in a typical office environment.

## 2 Measurements

### 2.1 Environment

The channel measurement campaign was carried out at the Université catholique de Louvain (UCL), Belgium, in winter 2016. The investigated environment was consisted of typical offices along a corridor separated by brick or plasterboard walls, as shown in Figure 1. Distances between the

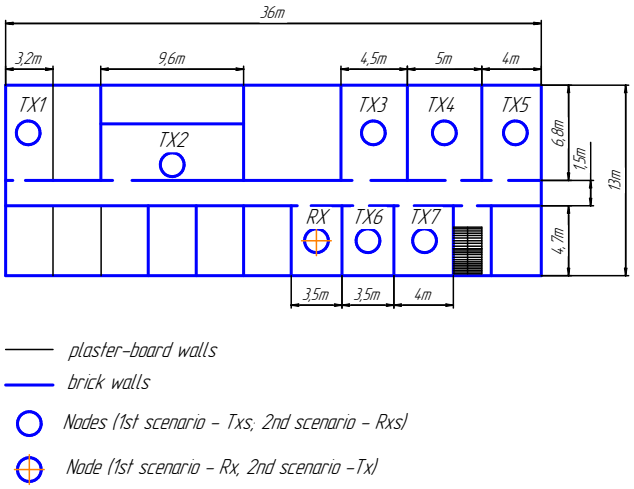


**Figure 1.** Floor-plan of peer-to-peer measurements

nodes were $21, 11, 4, 8, 7.5, 11, 15$ m. First, the receiver (Rx) (additionally marked with a cross) was located in a room in the middle of the building. The mobile transmitter (Tx) was successively positioned in different rooms along the corridor. For this measurements, the transmitter was moving in arbitrary directions with the speed $v \approx 1$ m/s only over an area of ($\sim 1$ m$^2$). Second, the same measurements were repeated for the case when the mobile Tx was in the room marked with a cross and static Rx was sequentially positioned in different rooms. In total, fourteen SIMO channels were measured.

### 2.2 Equipment

The measurements were carried out at 3.8 GHz over an effective bandwith of 120 MHz by means of UCL/ULB Elektrobit PROPSound™ channel sounder. A Uniform Circular Antenna (UCA) and a custom-made dipole (gain of 1.75 dB) antennas were used at the Rx and Tx, respectively. The RF cables had excellent RF stability, even when they were slightly bent or moved during the measurements. The channel transfer function (obtained from the impulse response) is denoted by $H[t, f, m]$, where $t$ denotes the time index, $f$ denotes the frequency index, and $m$ denotes the link index (one link joining a Tx-Rx pair). Initialization and Search Improved SAGE (ISIS) algorithm presented [4]

was used to estimate directional properties of the measured SIMO channels.

## 2.3 Concepts of Data Analysis

Similarly to [3, 2, 5], the average received power is defined as

$$\bar{P} = \frac{1}{T_s F M} \sum_{m=1}^{M} \sum_{t=1}^{T_s} \sum_{f=1}^{F} |H[t,f,m]|^2, \quad (1)$$

where $t, f$ and $m$ denote time sample, frequency tone and link nimber, respectively.

Using a sliding time window length $T_{av}$ of 1.6 s (corresponding to 20 wavelengths) to define the time-variant channel components, the time-variant average power of a narrowband channel (for each frequency bin with bandwidth equal $F_{coh,min} = 1/\tau_{max} = 4$ MHz) can be written as

$$P[t] = \frac{1}{T_{av} M} \sum_{t'=t-T_{av}/2}^{t+T_{av}/2} \sum_{m=1}^{M} |H[t',m]|^2 \quad (2)$$

The narrowband small-scale fading $G$ is then given by ($g = |G|$ being the amplitude):

$$G[t] = \frac{H[t]}{\sqrt{P[t]}}. \quad (3)$$

# 3 Experimental Characterization of Stationarity Period

## 3.1 Calculation of Correlation Matrices

Since SIMO channels were measured, we will concentrate our analysis on the Rx spatial correlation matrices. First, we define the minimum stationarity region. Based on the maximum observed delay spread of $\tau_{max} = \sim 250$ ns, the coherence bandwidth is estimated to be $F_{coh,min} = 1/\tau_{max} = 4$ MHz ($n_{f.coh} = 10$ frequency chips), therefore, within 120 MHz, there are only 30 independent frequency realizations, which means that effectively a smaller number of independent samples is available. Since the Rx and the scatterers are fixed, we obtain a maximal Doppler shift $f_{max} = 12.7$Hz. This results in a minimal coherence time $T_{coh,min} = 1/f_{max} = 7.9$ ms. It turns out that the detection of stationarity regions for all measured channels is possible for the window of $n_t = 40$ (approximately equivalent to a traveled distance of $5\lambda$). Consequently, we obtain estimates of the correlation matrices by averaging over $n_t \times n_f = 12000$ ($5 \times 30$ non-coherent) realizations. Hence, the time-variant correlation matrix $R_{Rx}(t)$ can be calculated as

$$R_{Rx}(t) = \frac{GG^H}{n_t \cdot n_f}, \quad (4)$$

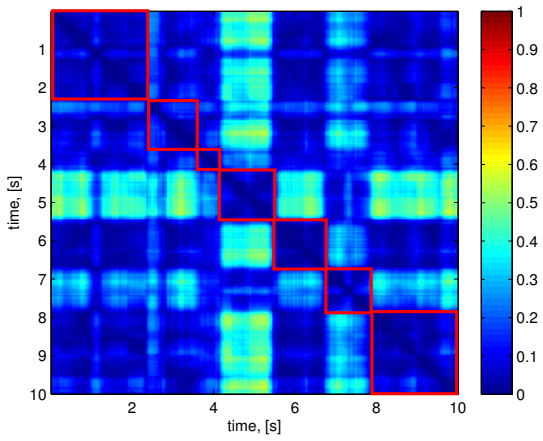


**Figure 2.** Correlation Matrix Distance for 10 seconds of measured channel Tx-Rx6, squared definition of stationarity periods

where $G$ is a data matrix with dimensions of $n_{antennas} \times (n_t \cdot n_f)$, where each column corresponds to the used time-frequency data block. These time-variant matrices are used for estimation of stationarity periods of the measured channels.

## 3.2 Calculation and Analysis of CMD

The Correlation Matrix Distance (CMD) was introduced [6, 7, 8] as a metric for the characterization of the change between two arbitrary spatial correlation matrices. Let us consider two spacial correlation matrices $R$ and $\hat{R}$, then the correlation matrix distance between the matrices can be expressed as

$$d_{corr} = 1 - \frac{\mathbf{tr}\{R\hat{R}\}}{\|R\|_F \|\hat{R}\|_F}, \quad (5)$$

where $\mathbf{tr}\{\cdot\}$ and $\|\cdot\|_F$ are the trace operator and the Frobenius norm, respectively. The CMD ranges between zero when the compared spatial correlation matrices are identical (up to a scaling factor) and one when they are completely different (i.e. uncorrelated). Hence, the correlation matrix distance between $R_{Rx}(t_i)$ and $R_{Rx}(t_j)$ can be used as a measure of non-stationarity, where $R_{Rx}(t_{i,j})$ are the correlation matrices calculated with (4) for time instants $i, j = 1 \ldots T_s - n_t$. A channel is considered to be stationary over a region (a traveled distance, time period, frequency range etc.) if the CMD is bellow the 0.2 threshold. In Figure 2 these time periods are indicated by red squares of sizes $n_{st.per} \times n_{st.per}$. Note, that the minimum duration of stationarity period equals $n_{st.per} = 80$ samples $= 0.8$ s (equivalent to the traveled distance of $\sim 10\lambda$). Next, blocks of $n_{st.per} \times n_{f.coh} \times n_{antennas}$ can be used to extract time-variant statistics of narrowband Second Order Scattering Fading (SOSF) SIMO channels.

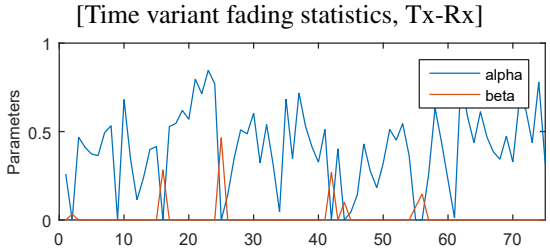


**Figure 3.** Typical variation of small-scale fading parameters over time for Tx1-Rx

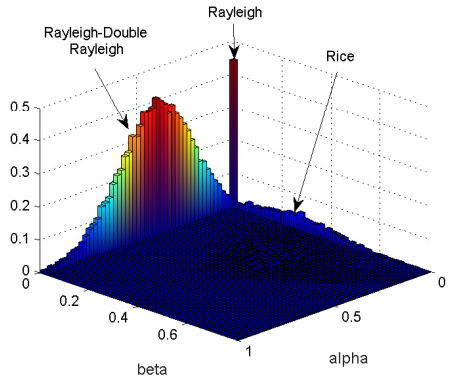


**Figure 4.** Probability density functions of the SOSF distribution parameters

## 4 Experimental Characterization of Non-Stationary Fading Statistics

### 4.1 SOSF Parameters Extracted From Measurement

Analogously to [3], SS fading over time can be described by a single distribution including a weighted combination of a Line-of-Sight (LOS) component, a Rayleigh fading component and a Double Rayleigh (DR) fading component. The probability density function of this kind of SS fading is given, as shown in [2, 3, 9], by the so-called SOSF distribution. This distribution can be described by only two parameters [10] $\alpha$ and $\beta$ characterizing the impact of the DR and LOS components, respectively. By iteratively fitting the SOSF probability density function to the experimental fading distributions (assuming a moment-based estimate as starting point [10]) temporal behavior of the parameters are estimated (see Figure 3). We observe that predominantly Rayleigh - Double Rayleigh (RDR) fading ($\beta = 0, 0 < \alpha < 1$) occurs as in [3]. Only scarcely we observe an impact of LOS (Rice and Double Rayleigh and Line-of-Sight (DRLOS)).

In Figure 4, three main groups (Rice, Rayleigh, Rayleigh-Double Rayleigh) can be observed. These subsets of SOSF describe the major part of measured SS fading realizations. For reasons of simplicity, we neglect DRLOS and points in the middle zone (where $0 < \alpha < 1, 0 < \beta < 1$ and $\alpha + \beta \neq 1$). The distribution of the parameter $\alpha$ for the RDR subset is found to be well approximated by the Beta distribution. The distribution of the K-Factor in Rician fading, $K = \frac{\beta}{1-\beta}$, can be modeled by Extreme Value distribution, when the K-factor expressed in decibels.

**Table 1.** Evaluated parameters of the SOSF distribution

| Subset | Distribution Parameters | $\tau$ |
|---|---|---|
| Rician | $K \sim p_{ev}(-3.1, 3), \alpha = 0$ | $\tau_K = 0.8s$ |
| RDR | $\alpha \sim p_\beta(3, 4.2), \beta = 0$ | $\tau_\alpha = 2.4s$ |
| Rayleigh | – | – |

**Table 2.** Probability and Transition matrices

| Subset | Probability | Rician | RDR | Rayleigh |
|---|---|---|---|---|
| Rician | 0.12 | 0.19 | 0.10 | 0.12 |
| RDR | 0.83 | 0.75 | 0.85 | 0.81 |
| Rayleigh | 0.05 | 0.06 | 0.05 | 0.07 |

Eventually, a probability distribution of the SOSF parameters within the subset can be estimated (see Table 1). Note that the autocorrelations of $\alpha$ and $K$ are decreasing exponential functions with the decay times $\tau_{K,\alpha}$, respectively. Table 2 presents the probabilities of the subsets and probability of the transitions between different kinds of SS fading. Note, that i) a high probability of occurrence for RDR fading is observed as in [3], ii) $\beta$ can be obtained as $\beta = \frac{K}{1+K}$.

### 4.2 Directional Statistics

Figure 5 shows Angle of Arrival (AoA) extracted from the measurements. Two situations can be differentiated: when the nodes are on the same and opposite sides of the corridor. When the corridor is a part of the propagation channel, the major part of waves arrives over a smaller angular range. Usually, the direction of arriving waves corresponds to a corner of the room where the Rx is located. In the case when the nodes are located in the rooms on the same side of the corridor, AoA are dispersed over a larger range, mostly concentrated in the direction of the Tx. Moreover, a noticeable impact of the backscattering is observed. The distribution of measured AoAs can be approximated by a mixture of Tikhonov-von Mises (TvM) distributions:

$$p_{TvM}(x, w, \kappa_1, \kappa_2) = w \cdot \frac{e^{(\kappa_1 \cos(x))}}{2\pi I_0(\kappa_1)} + (1-w) \cdot \frac{e^{(\kappa_2 \cos(x-\pi))}}{2\pi I_0(\kappa_2)}, \quad (6)$$

where $I_0$ is the modified Bessel function of order 0, $\kappa$ and $\mu$ are measures of concentration and location, respectively. Weights $w$ and $(1-w)$ describe the impacts of components. Let us separate analysis and modeling of two different situations mentioned above.


**Figure 5.** Angular Power Spectrum Top: Rx is in the same room, bottom: Rx is in different rooms

**Table 3.** Evaluated parameters of angular distributions

| Parameter | Same side | Different sides |
|---|---|---|
| $\kappa_1$ | $p_\Gamma(16.1, 0.13)$ | $p_\Gamma(7, 0.7)$ |
| $\kappa_2$ | $p_\Gamma(20.8, 0.11)$ | $p_\Gamma(7, 0.17)$ |
| $w$ | $p_\beta(23, 13.6)$ | $p_\beta(8.8, 14.8)$ |
| $c_{\kappa_1,\kappa_2}$ | $-0.28$ | $-0.54$ |
| $c_{\kappa_1,w}$ | $-0.78$ | $-0.84$ |
| $c_{\kappa_2,w}$ | 0.37 | 0.66 |

In Figure 5 (Rx (Tx) 5) we can see a peak pointing towards the transmitter. The peak can be modeled as a Tikhonov-von Mises distribution with a large parameter $\kappa_1$ and the mean direction $\mu_1$. Up to seven small peaks can be detected in the measurements, but modeling of all these components is not practical. For sake of simplicity, the distribution of AoA excluding the main peak can be approximated by single TvM distribution with a small parameter $\kappa_2$. The mean angle of this component has low impact because the distribution is close to uniform when $\kappa_2$ is small. In the case of the same-side rooms, again main peaks pointing towards the transmitter are seen in Figure 5 (Rx (Tx) 6). However, the peak is wider and its impact is just slightly bigger than the one of backscattering. Hence, the final distribution can be approximated by two TvM distributions with parameters $\kappa_1$ and $\kappa_2$ and $|\mu_1 - \mu_2| = \pi$. To estimate the parameters $\kappa_1, \kappa_2$, we assume that the angle corresponding to the maximum of AoA distribution is the direction of LOS and shifted to 0. Consequently, $\mu_1 = 0$ and, considering the reasoning above, we can set $\mu_2 = \pi$. Next, we performed least squares fitting of the measured distributions and the Kolmogorov-Smirnov test with 95 % confidence interval was used to check whether the LS estimation gives an appropriate result. It turns out that $\kappa_{1,2}$ follow Gamma distributions and some correlation between the parameters was found. Parameter $w$ is Beta-distributed. The temporal autocorrelation of the parameters $\kappa_1, \kappa_2, w$ is a decreasing exponential function with the decay time of 2.4 s ($\approx$ 3 stationarity periods). The evaluated parameters are listed in Table 3.

## 5 Conclusions

This paper has presented an analysis of time-variant statistics of a peer-to-peer SIMO channels based on measurement in an indoor office environment at 3.8 GHz: i) Analysis of measured Rx spatial correlation matrices shows that the minimum stationarity period equals 0.8 s, ii) Distribution of angles of arrival can be described by a bimodal Tikhonov-von Mises distribution with time-variant parameters Gamma ($\kappa_1, \kappa_2$) and Beta ($w$) distributed, iii) Distributions of the parameter $\alpha$ can be modeled by Beta distribution, iv) Distribution of the K-Factor can be well approximated by Extreme Value distribution.

## References


[1] Cisco, "Cisco visual networking index: Global mobile data traffic forecast update, 2016-2021," Tech. Rep.

[2] C. Oestges et al., "Experimental characterization and modeling of outdoor-to-indoor and indoor-to-indoor distributed channels," *IEEE Trans. on Vehicular Technology*, vol. 59, no. 5, pp. 2253–2265, June 2010.

[3] E. Vinogradov et al., "Measurement-based modeling of time-variant fading statistics in indoor peer-to-peer scenarios," *IEEE Trans. on Antennas and Propagation*, vol. 63, no. 5, pp. 2252–2263, May 2015.

[4] B. H. Fleury et al., "High-resolution channel parameter estimation for mimo applications using the sage algorithm," in *International Zurich Seminar on Broadband Communications, Access, Transmission, Networking*, 2002, pp. 30–1–30–9.

[5] E. Vinogradov, "Multi-dimensional radio channel models for indoor distributed communications," Ph.D. dissertation, 2017.

[6] M. Herdin, "Non-stationary indoor MIMO channels," Ph.D. dissertation, Technischen Universität Wien, 2004.

[7] M. Herdin et al., "Correlation matrix distance, a meaningful measure for evaluation of non-stationary MIMO channels," *IEEE 61st Vehicular Technology Conference*, vol. 1, pp. 136 – 140, June 2005.

[8] H. Xiao and A. G. Burr, "Full channel correlation matrix of a time-variant wideband spatial channel model," *IEEE PIMRC*, pp. 1 – 5, Sep. 2006.

[9] J. Salo et al., "Statistical analysis of the multiple scattering radio channel," *IEEE Trans. on Antennas and Propagation*, vol. 54, no. 11, pp. 3114–3124, November 2006.

[10] B. Bandemer et al., "Physically motivated fast-fading model for indoor peer-to-peer channels," *Electronics Letters*, vol. 45, no. 10, pp. 515–517, May 2009.